Human Interleukin-10 Gene Transfer Is Protective in a Rat Model of Parkinson's Disease

Louisa C Johnston[1], Xiaomin Su[2,4], Kathleen Maguire-Zeiss[2,3,*], Karen Horovitz[1], Irina Ankoudinova[5], Dmitry Guschin[5], Piotr Hadaczek[1], Howard J Federoff[2,3,*], Krystof Bankiewicz[1] and John Forsayeth[1]

*[1]Department of Neurosurgery, University of California San Francisco, San Francisco, California, USA; [2]Center for Aging and Developmental Biology, Institute for Biomedical Research, University of Rochester School of Medicine and Dentistry, Rochester, New York, USA; [3]Department of Neurology, University of Rochester School of Medicine and Dentistry, Rochester, New York, USA; [4]Department of Microbiology and Immunology, University of Rochester School of Medicine, Rochester, New York, USA; [5]Sangamo BioSciences Inc., Richmond, California, USA; *Current address: Department of Neurology, Georgetown University Medical Center, Washington, District of Columbia, USA; Office of the Executive Vice President and Executive Dean, Georgetown University Medical Center, Washington, District of Columbia, USA*

In Parkinson's disease (PD) chronic inflammation occurs in the substantia nigra (SNc) concurrently with dopaminergic neurodegeneration. In models of PD, microglial activation precedes neurodegeneration in the SNc, suggesting that the underlying pathogenesis involves a complex response in the nigrostriatal pathway, and that the innate immune system plays a significant role. We have investigated the neuroprotective effect of an adeno-associated viral type-2 (AAV2) vector containing the complementary DNA (cDNA) for human interleukin-10 (hIL-10) in the unilateral 6-hydroxydopamine (6-OHDA) rat model of PD. AAV2-hIL-10 reduced the 6-OHDA-induced loss of tyrosine hydroxylase (TH)-positive neurons in the SNc, and also reduced loss of striatal dopamine (DA). Pretreatment with AAV2-hIL-10 reduced glial activation in the SNc but did not attenuate striatal release of the inflammatory cytokine IL-1β. Assessment of rotational behavior in response to apomorphine challenge showed absence of asymmetry, confirming protection of dopaminergic innervation of the lesioned striatum. At baseline, 6-OHDA-lesioned animals displayed a deficit in contralateral forelimb use, but pretreatment with AAV2-hIL-10 reduced this forelimb akinesia. Transcriptional analyses revealed alteration of a few genes by AAV2-hIL-10; these alterations may contribute to neuroprotection. This study supports the need for further investigations relating to gene therapies aimed at reducing neuroinflammation in early PD.

Received 23 January 2008; accepted 28 April 2008; published online 10 June 2008. doi:10.1038/mt.2008.113

INTRODUCTION

A growing body of evidence supports the concept that activated glia play a critical role in the degeneration of nigral dopaminergic neurons in Parkinson's disease (PD). Activated microglia secrete a complex array of cytokines, chemokines, proteolytic enzymes, reactive oxygen/nitrogen species and complement proteins that may have deleterious effects on the dopaminergic system.[1] Interestingly, α-synuclein, found in nigral neurons and strongly implicated in PD, has been shown to activate microglia,[2,3] suggesting an underlying mechanism that links chronic neuroinflammation with PD.[2] There is also at least one report that suggests that inflammatory factors released from microglia promote α-synuclein accumulation.[4]

Although it is clear that cellular manifestation of neuroinflammation takes place in the substantia nigra (SNc) of PD patients and animal models, it has not yet been unequivocally demonstrated whether this is an active process that contributes to dopaminergic neuron death, or whether it merely represents a response to the ongoing neuronal cell death. However, it is important to note that both 1-methyl-4-phenyl-1,2,3,6-tetrahydropyridine and 6-hydroxydopamine (6-OHDA) induce activation of microglia in the SNc, and that this activation precedes the demise of dopaminergic neurons. It has been shown that anti-inflammatory drugs that reduce microglial activation (*e.g.*, minocycline) are somewhat efficacious in protecting nigral dopaminergic neurons.[5] However, the anti-inflammatory action of certain cytokines has not been explored in these models.

The anti-inflammatory cytokine, interleukin-10 (IL-10), is a homodimeric, pleiotropic cytokine that was originally described as a cytokine inhibitory factor. It can antagonize the actions of the major inflammatory cytokines. Biologically active IL-10 protein is expressed in the central nervous system by monocytes, astrocytes, and microglia, and attenuates the lipopolysaccharide (LPS)-induced expression of proinflammatory cytokines and the induction of neuroapoptosis.[6–9] IL-10 appears to act as an antiapoptotic agent by blocking the actions of caspase-3 (ref. 8), decreases microglial activation in response to inflammatory cytokine exposure, and inhibits microglial stimulation of $CD4^+$ T cells.[10] IL-10 reduces LPS-induced neurotoxicity *in vitro* through a mechanism that involves inhibition of nicotinamide adenine dinucleotide phosphate oxidase activity.[5,11] Importantly, although IL-10 failed to be protective in the LPS model of acute neurodegeneration after a single nigral injection, neuroprotection was observed after 14 days of continuous recombinant IL-10 delivery.[8] We therefore proposed that sustained administration of IL-10 cytokine in a viral vector

Correspondence: *John R. Forsayeth, Department of Neurosurgery, 1855 Folsom Street, MCB 226, University of California San Francisco, San Francisco, California 94103-0555, USA. E-mail: john.forsayeth@ucsf.edu*

platform might provide significant protection of nigral dopaminergic neurons in a rodent model of PD.

In this study we found that IL-10, when delivered intrastriatally by means of an adeno-associated viral (AAV) vector, protected nigral neurons against intrastriatally infused 6-OHDA. Protection was seen at the behavioral, biochemical, and histological levels. The efficacy of the IL-10 vector platform demonstrated here suggests that further exploration of this approach as a therapeutic strategy for PD would prove useful.

RESULTS

In order to determine whether human IL-10 (hIL-10) expression can protect nigral neurons against 6-OHDA, we infused rats intrastriatally by convection-enhanced delivery (CED), first with AAV2-hIL-10 or a control vector, AAV2-GFP, and then 3 days later with either 20 µg 6-OHDA or saline. Our method differs from earlier 6-OHDA lesion techniques in that the toxin was infused slowly under pressure into the striatum by CED rather than injected as a bolus into the striatum.[12] This regimen resulted in four groups of test and control animals. In our experience, detectable (but not maximal) expression of transgene can be seen within 1–2 days after transduction.[13]

In an initial experiment, we confirmed expression by infusing the rat striatum bilaterally with 1×10^{11} vector genomes of AAV2-hIL-10. This infusion directed a rapid increase in the IL-10 content in the striatum, reaching a level of 57.98 ± 14.8 pg of hIL-10/mg protein after 3 days (**Figure 1**, $n = 4$). It should be noted that the enzyme-linked immunosorbent assay (ELISA) for hIL-10 does not detect rat IL-10, and hIL-10 is not detected in untreated control tissue. As a positive control, recombinant hIL-10 (0.5 µg) was infused into the striata of rats ($n = 4$), and tissue was harvested only 3 hours later (data not shown). The low residual level of recombinant protein (11.43 ± 2.1 ng/mg tissue) measured using ELISA reflects the rapid metabolic clearance of IL-10.[14] We also determined whether hIL-10 was produced in an area containing neurons that project to the striatum. Mean levels of hIL-10 in the ventral mesencephalon were comparable to those in the striatum by 28 days after infusion (data not shown).

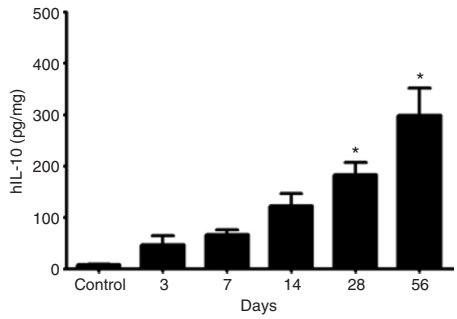

Figure 1 Human interleukin-10 (hIL-10) secretion in rat brain after striatal infusion of AAV2-hIL-10. The amount of hIL-10 in the striatum was determined using enzyme-linked immunosorbent assay. The X-axis shows number of days after vector infusion. hIL-10 was measured in whole striatum ($n = 4$/time point). Samples were run in duplicate. The data are expressed as pg/mg of protein (mean value ± SEM, $n = 4$). Statistical differences were measured using one-way analysis of variance and Newman–Keuls multiple test: *$P < 0.05$ versus control rats. AAV2, adeno-associated virus type-2.

Behavior

Unilaterally lesioned rats turned contralaterally to the lesioned hemisphere if challenged with subcutaneous apomorphine, a dopamine (DA) receptor agonist. Sham-lesioned rats did not rotate in response to apomorphine (**Figure 2a**). 6-OHDA-lesioned rats infused with AAV2-GFP turned contralaterally with >15-turns/5 minutes at peak effect. In contrast, rats infused with AAV2-hIL-10 did not show significant contralateral turning response.

In the step-adjustment test, there was found to be a significant impairment in contralateral, left-paw performance in lesioned rats treated with AAV2-GFP and 6-OHDA, but no impairment in the ipsilateral right paw (**Figure 2b**). The decrease in the number of adjusting steps made by the left paw was seen in both the forehand and backhand directions (data shown only for the forehand). There was a small decrease over time in right-paw performance in sham-lesioned animals, suggesting habituation.[15] A pronounced protective effect of AAV2-hIL-10 was seen

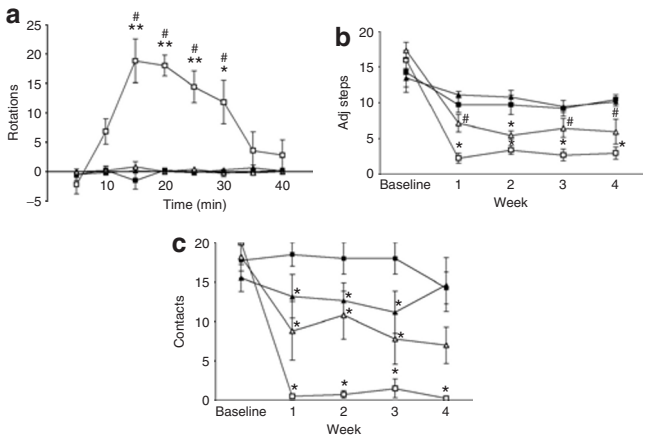

Figure 2 Infusion with AAV2-hIL-10, but not AAV2-GFP, prior to lesion with 6-OHDA reduces denervation sensitivity and forelimb akinesia. Symbol key: black squares (AAV2-GFP), black triangles (AAV2-hIL-10), white squares (AAV2-GFP/6-OHDA), and white triangles (AAV2-hIL-10/6-OHDA). (**a**) Apomorphine-induced rotational asymmetry: the data represent the number of contralateral rotations (minus ipsilateral rotations) in 5-minute intervals after administration of apomorphine (0.05 mg/kg subcutaneously). *$P < 0.05$ (two-way analysis of variance (ANOVA) followed by Bonferroni tests); comparisons were made with the respective sham-lesioned groups. (**b**,**c**) Human interleukin-10 (hIL-10), but not green fluorescent protein (GFP), reduced forelimb akinesia resulting from unilateral 6-hydroxydopamine (6-OHDA) lesion. (**b**) Step-adjustment test: data are shown as the mean (± SEM) number of adjusting steps for the left forelimb in the forehand direction ($n = 4$–6/group). Effect of time, treatment, and interaction between these factors: $P < 0.0005$ (two-way ANOVA). *$P < 0.05$ (one-way ANOVA); comparisons were made with the respective sham-lesioned controls using Newman–Keuls tests. #AAV2-hIL-10/6-OHDA vs. AAV2-GFP/6-OHDA, $P < 0.05$. Right forelimb data revealed a small decrease in the mean number of steps over time. However, this decrease is comparable to previous reports of habituation using this test. (**c**) Cylinder test: data are shown for the mean (±SEM) number of full left paw contacts. Effect of time, treatment and interaction between these factors: P values <0.005 (two-way ANOVA). *$P < 0.05$ compared to AAV2-GFP/sham-treated animals (one-way ANOVA with Newman–Keuls tests for comparisons). Data for the right paw revealed a decrease in wall contacts in the sham-lesioned AAV2-hIL-10 group, but performance returned to normalcy by the end of the experiment. In AAV2-GFP/6-OHDA rats right paw contacts had decreased by 60% at 28 days (data not shown). AAV2, adeno-associated virus type-2; adj steps, adjusting steps.

($P < 0.05$) in comparison with lesioned AAV2-GFP-lesioned 6-OHDA rats.

In the cylinder test, AAV2-GFP-treated rats displayed a significant decrease in the number of contacts made by the contralateral, but not the ipsilateral, left paw 1 week after 6-OHDA infusions that persisted up to 28 days (**Figure 2c**). As for the step-adjustment test, a clear protective effect of AAV2-hIL-10 was seen in comparison with the 6-OHDA lesioned AAV2-GFP-treated animals. However, the degree of protection provided by IL-10 did not reach statistical significance.

Neurochemistry

Bilateral striatal infusion with AAV2-hIL-10 3 days prior to 6-OHDA infusion into the right striatum reduced the 6-OHDA-induced loss of striatal DA and its metabolites seen after pretreatment with the control transgene AAV2-GFP (**Figure 3**). Furthermore, AAV2-hIL-10 also reduced the 6-OHDA-induced increase in striatal DA turnover (**Figure 3** inset). These data indicate that the protective effect of hIL-10 on behavior was mediated through a partial preservation of basal striatal DA levels.

Immunohistochemistry

The number of tyrosine hydroxylase (TH) immunoreactive neurons in the SNc was unaffected by sham-lesioning in rats that had previously received AAV2-GFP (**Figure 4a** and **e**) or AAV2-hIL-10 (**Figure 4b** and **e**). TH immunostaining revealed dopaminergic cell loss in the SNc 1 month after infusion of 20 µg 6-OHDA (**Figure 4c** and **e**). AAV2-hIL-10 infusion reduced the loss of TH-immunoreactive neurons in the SNc 28 days after lesion (**Figure 4d** and **e**). This degree of protection was found to be greater than the effect of IL-10 expression on striatal DA levels. In this model, therefore, it would seem that partial protection of nigrostriatal neurons is required in order to gain a great improvement in motor function.

In sham-lesioned rats there was little immunoreactivity in respect of membrane attack complex-1 (MAC-1) in the SNc (**Figure 5a**). In AAV2-GFP rats, 1 month after infusion of 6-OHDA a subpopulation of MAC-1 immunoreactive microglia in the SNc displayed activated morphology characterized by amoeboid shape, enlarged cell bodies, and both shortening and thickening of their normally ramified processes (**Figure 5c** and **f**). Activated microglia were also observed in the contralateral SNc. In contrast, in 6-OHDA

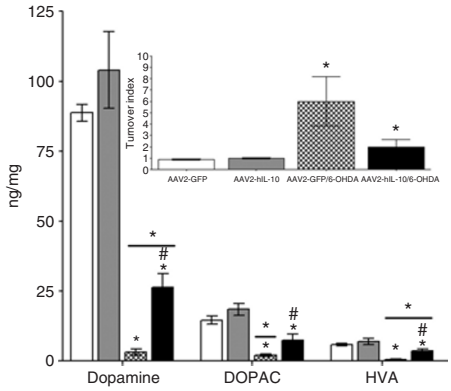

Figure 3 Effect on dopamine deficiency in precommissural striatum caused by infusion with AAV2-hIL-10 or AAV2-GFP prior to 6-hydroxydopamine (6-OHDA) lesion of the right striatum. White bars, AAV2-GFP/sham ($n = 4$); grey bars, AAV2-hIL-10/sham ($n = 6$); hatched bars, AAV2-GFP/6-OHDA ($n = 5$); and black bars, AAV2-hIL-10/6-OHDA ($n = 5$). Mean (±SEM) values are expressed as ng/mg of total protein. Data are shown only for the right striatum. Left striatum values were comparable to those of sham-treated right striatum, and are in agreement with previously published values for the rat.[50] Two-way ANOVA analysis of dopamine, dihydroxyphenylacetic acid (DOPAC), and homovanillic acid (HVA) data: effect of hemisphere $P < 0.0001$, effect of treatment $P < 0.0005$, and interaction between hemisphere and treatment $P < 0.0001$. Small $^{*}P < 0.005$, as compared to sham-lesioned groups, and $^{\#}P < 0.05$ as compared to AAV2-GFP/6-OHDA lesion group; Newman–Keuls tests. Large $^{*}P < 0.01$ compared to left striatum within treatment groups; paired two-tailed *t*-test. AAV2, adeno-associated virus type-2; ANOVA, analysis of variance; GFP, green fluorescent protein; hIL-10, human interleukin-10.

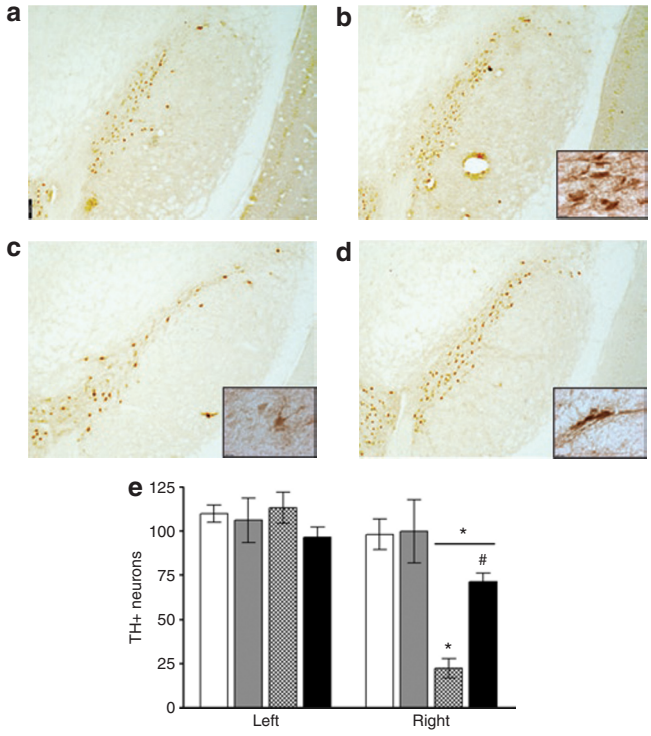

Figure 4 Tyrosine hydroxylase immunoreactive nigral neurons in substantia nigra compacta (SNc) 28 days after infusion of 6-hydroxydopamine (6-OHDA). White bars, AAV2-GFP/sham; grey bars, AAV2-hIL-10/sham; hatched bars, AAV2-GFP/6-OHDA; and black bars, AAV2-hIL-10/6-OHDA. Striata were infused bilaterally with adeno-associated virus type-2 (AAV2) constructs (10^{11} vector genomes/20 µl/side) containing a gene for either human interleukin-10 (hIL-10) or green fluorescent protein (GFP). Three days later the right striatum was infused with 20 µg of 6-OHDA or vehicle (sham-lesion). (**a**) AAV2-GFP/sham; (**b**) AAV2-h IL-10/sham; (**c**) AAV2-GFP/6-OHDA; (**d**) AAV2-h IL-10/6-OHDA. Scale-bar = 300 µm (×2.5 original magnification); (**e**) mean values are shown for the intact (left) and lesioned (right) SNc at the level of the accessory optic tract ($n = 4$–6/group). Bars represent total number of tyrosine hydroxylase (TH)-immunoreactive neurons. Right hemisphere data: small $^{*}P < 0.001$; two-way analysis of variance (ANOVA) followed by Newman–Keuls post-tests, comparisons made with sham-lesioned group. $^{\#}$AAV2-h IL-10/6-OHDA compared with AAV2-GFP/6-OHDA $P < 0.01$; one-way ANOVA followed by Newman–Keuls *post hoc* test. Large $^{*}P < 0.01$ compared to left side within treatment groups; paired two-tailed *t*-test. Scale bar = 12 µm (×100 magnification).

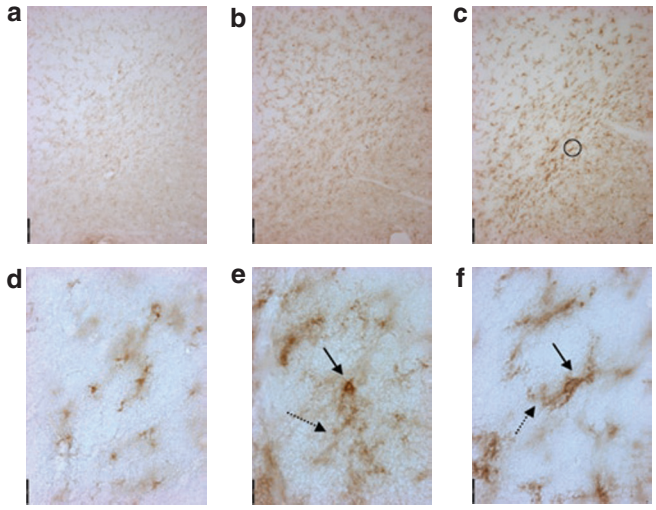

Figure 5 Membrane attack complex-1 immunoreactive microglia in the substantia nigra compacta of 6-hydroxydopamine (6-OHDA)-lesioned and sham-lesioned animals 28 days after injection. Little immunoreactivity was observed in sham-lesioned rats and no difference was observed between these groups. Images are shown only for the right striatum. The degree of activation induced by the 6-OHDA lesion was modulated by the combined AAV2 treatment. (**a**,**d**) AAV2-GFP/sham, (**b**,**e**) AAV2-hIL-10/6-OHDA, (**c**,**f**) AAV2-GFP/6-OHDA (n = 4–6/group). Scale bars = (**a–c**) 120 µm (×10 magnification), (**d–f**) 12 µm (×100 magnification). AAV2, adeno-associated virus type-2; GFP, green fluorescent protein.

Table 1 AAV2-hIL-10 attenuates astrogliosis in the rat SNc 28 days after 6-OHDA infusion

	Control	AAV2-GFP	AAV2-hIL-10	AAV2-GFP/6-OHDA	AAV2-hIL-10/6-OHDA	LPS
Left	0	0	0-+	0-+	+	+
Right	0	0	0-+	+++-++++	+-++	++++

Abbreviations: AAV2, adeno-associated virus type-2; GFP, green fluorescent protein; hIL-10, human interleukin-10; 6-OHDA, 6-hydroxydopamine; SNc, substantia nigra compacta.
Lipopolysaccharide (LPS) (10 µg) induced astrogliosis 24 hours after supra-nigral microinjection. Control samples were from untreated or sham-lesioned (no vector) rats. Ratings were performed blind by two independent observers.

rats pretreated with AAV2-hIL-10, MAC-1-positive microglia had more ramified processes and smaller cell bodies (Figure 5b and e).

One month after sham-lesion, rats that had received AAV2-GFP displayed no evidence of astrogliosis in the SNc and were indistinguishable in this respect from naive animals (Table 1). In contrast, sham-lesioned animals that received AAV2-hIL-10 showed mild astrogliosis in the SNc. One month after 6-OHDA infusion, astrogliosis was observed in the ipsilateral SNc of AAV2-GFP/6-OHDA rats comparable to that seen in rat SN microinjected with LPS 24 hours earlier. A dense population of astroglia with enlarged cell bodies and thickened processes was seen, covering most of the area of the SNc. In contrast, 6-OHDA rats that had received AAV2-hIL-10 did not exhibit similar astrogliosis.

Striatal inflammation

Inflammation in the brain is accompanied by a sharp rise in inflammatory cytokines, chiefly IL-1β.[5,7] Rat IL-1β was not detected in the striata of control rats or in the intact, contralateral striata of

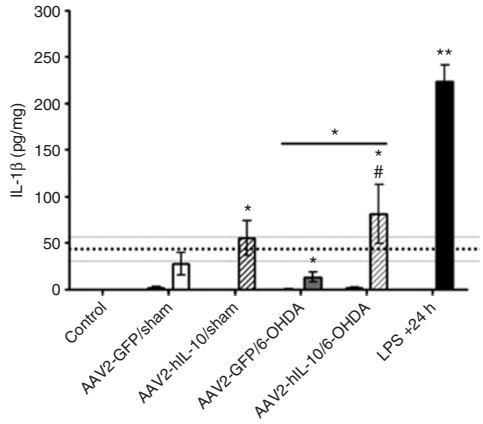

Figure 6 6-Hydroxydopamine (6-OHDA)-induced increase in rat striatal interleukin-1β (IL-1β) and the effect of adeno-associated viral type-2 (AAV2) vectors. Rats were killed 7 days after 6-OHDA-lesion or sham-lesion. The data are expressed as mean ± SEM values and reported in pg/mg of total protein, n = 4/group. Statistical differences were measured using one-way analysis of variance (ANOVA) ($P < 0.0001$) followed by Bonferroni post-tests. *$P < 0.025$ or **$P < 0.005$: for right versus left striatum, paired t-tests were used. One-way ANOVA followed by Newman–Keuls tests: $^{\#}P < 0.05$ AAV2-hIL-10/6-OHDA compared with control transgene 6-OHDA rats. Large *$P < 0.05$: IL-1β levels in all treatment groups were significantly reduced in comparison with lipopolysaccharide (LPS)-treated animals ($P < 0.005$). Broken line indicates the saline sham-lesion effect, as given by the mean (thick broken line; 43 pg/mg) for all sham-lesioned animals, ±SEM (thin broken lines, (12). hIL-10, human IL-10.

treated rats (Figure 6). One week after sham-lesion with saline, IL-1β increased in the AAV2-hIL-10-infused striatum relative to the contralateral hemisphere. A similar increase occurred relative to the contralateral striatum after control vector infusion, but this effect did not achieve statistical significance because of scatter in the data and the small number of animals (n = 4). In order to generate a positive control we injected LPS into rat striatum, thereby evoking a large increase in striatal IL-1β 24 hours after injection. To our surprise, IL-1β in the striatum, measured at 7 days after 6-OHDA lesion, appeared to be greater in animals pretreated with AAV2-hIL-10 than in those pretreated with the control transgene. However, this increase was reduced by comparison to the LPS response and is not significantly increased by comparison to the sham-lesioning effect seen in AAV2-hIL10 rats (Figure 6). We have concluded that the IL-10-mediated neuroprotection in the SNc is unlikely to be mediated through suppression of inflammatory cytokine expression.

Gene expression profile and quantitative PCR in rat striatum

Next, we wanted to determine the acute effects of IL-10 on gene expression after 6-OHDA exposure with a global screen of gene expression. Striatal tissues were harvested at 3 days after the 6-OHDA lesion. The RNA derived from AAV2-GFP/6-OHDA treated animals was compared to that of AAV2-hIL-10/6-OHDA treated animals in an Affymetrix micro-array representing the entire rat genome. A number of transcripts involved in immune system function were upregulated in AAV2-hIL-10/6-OHDA relative to AAV2-GFP/6-OHDA rats (data not shown). It is

important to note that microarrays are not considered definitive because false-positive signals often appear in such screens. However, such arrays help to focus attention on candidate genes. Therefore, false-positives were eliminated by follow-up, confirmatory quantitative reverse transcriptase PCR to reveal a number of significant changes (**Figure 7**). The largest increase in expression occurred for IL-10, which was upregulated 40-fold on account of the human transgene and not the endogenous rat IL-10 (**Figure 7a**). The expression of the chemokine CCL5 (RANTES) was increased (**Figure 7b**), a change which could be neuroprotective to striatal terminals.[16,17] 6-OHDA decreased the expression of an important endothelial adhesion factor, carcinoembryonic antigen-related cell adhesion molecule 1, in control transgene rats, and AAV2-hIL-10 restored the expression to normal levels (**Figure 7c**). Gene expression of another chemokine, CXCL13, was also elevated by AAV2-hIL-10 pretreatment (**Figure 7d**). The astroglial S100 transcript was upregulated by 6-OHDA in control transgene-treated rats but not in AAV2-hIL-10-treated rats (**Figure 7e**). This is an interesting change, given that S100 appears to be a functional marker for astroglia and that its expression increases after neuronal damage.[18]

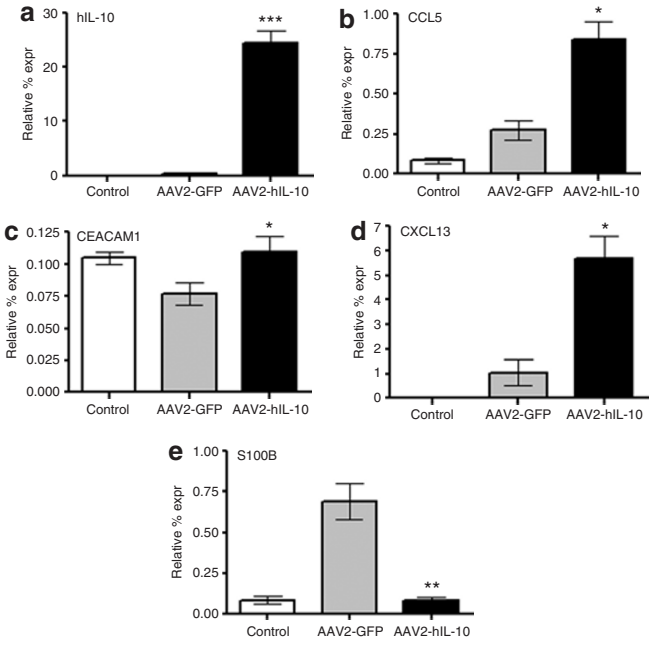

Figure 7 Acute changes in gene expression induced by 6-hydroxydopamine (6-OHDA) and modulation by the anti-inflammatory cytokine interleukin-10 (IL-10). (**a**) Human IL-10 (hIL-10), (**b**) CCL5, (**c**) CEACAM1, (**d**) CXCL13, and (**e**) S100B. Rats were infused with AAV2-GFP or AAV2-hIL-10 (n = 4/group). Three days later, 6-OHDA was infused. Striata (data shown for right side) were collected 3 days later. Control animals did not receive any infusions. The data are expressed as mean relative percentage expression (expr) values; normalized to the housekeeping gene for rat glyceraldehyde 3-phosphate dehydrogenase. Statistical differences were measured using t-tests *P < 0.05, **P < 0.005, ***P < 0.0005 for AAV2-hIL-10/6-OHDA rats as compared to control transgene 6-OHDA rats. AAV2, adeno-associated virus type-2; CCL5, chemokine (C-C motif) ligand 5; CEACAM1, carcinoembryonic antigen-related cell adhesion molecule 1; CXCL13, chemokine (C-X-C motif) ligand 13; GFP, green fluorescent protein; S100B, S100 calcium-binding protein B.

This finding concurs with our histological findings of reduced glial fibrillary–associated protein (GFAP) immunoreactivity in AAV2-hIL-10-pretreated 6-OHDA-lesioned rats, suggesting a shift in functional response of astroglia to 6-OHDA against a background of high striatal levels of the cytokine IL-10.

DISCUSSION

This study demonstrates that hIL-10 delivered by an AAV2 vector significantly preserves nigrostriatal function in rats 1 month after exposure to the neurotoxin 6-OHDA. Motor deficits typically seen in the model were ameliorated by hIL-10 expression. This study also extends previous findings from rotational tests with the CED 6-OHDA model to sensitive tests of forelimb akinesia. This represents an advantage of this model, given that microinjection of a similar amount of 6-OHDA induces only temporary and mild forelimb akinesia.[19,20]

We also report a loss of dopaminergic nigral neurons and striatal DA deficiency similar to those reported earlier.[13,19] Our results show that in the CED 6-OHDA-model, microglial and astroglial activation persists for 28 days after the initial insult. This has been documented in the traditional microinjection 6-OHDA model.[21] Long-term gliosis is a desirable feature of any experimental model of PD, and has been documented in 1-methyl-4-phenyl-1,2,3,6-tetrahydropyridine–exposed monkeys and humans, persisting for years after the initial insult.[22,23] The chronic microglial inflammation observed in the 6-OHDA model contrasts with the transient activation reported in rodent models using 1-methyl-4-phenyl-1,2,3,6-tetrahydropyridine and LPS.[24,25]

IL-10 reduced the nigral dopaminergic neuronal loss and striatal DA deficiency resulting from 6-OHDA lesion by ~50 and 20%, respectively. IL-10 also reduced the compensatory increase in DA turnover occurring after 6-OHDA exposure[26] (**Figure 3** inset). In parallel to these neurochemical changes, IL-10 attenuated both microglial and astroglial activation induced by the 6-OHDA insult. Microglial morphology was visualized with MAC-1 immunoreactivity, established as a marker of phagocytic activity.[27] In IL-10/6-OHDA rats the microglia were less activated, with thinner, more ramified processes and smaller cell bodies, consistent with IL-10's ability to elicit microglial ramification *in vitro*.[28,29] Microglia and astroglia secrete a number of factors, some of which promote neurodegeneration; nevertheless we did not observe an increase in the expression of proinflammatory cytokines 3 days after 6-OHDA lesion in control transgene rats. However, at 7 days after 6-OHDA infusion, we measured elevated striatal IL-1β levels by ELISA after infusion of either of the vectors in 6-OHDA-lesioned striata (**Figure 6**). Saline infusion alone produced a small increase in IL-1β within the striatum as compared to the contralateral hemisphere. But, the sham-induced increase in IL-1β did not have adverse degenerative effects on the nigrostriatal pathway. This might indicate a specific vector effect in stimulated IL-1β release; that is, an inflammatory reaction stimulated by viral particles. A similar increase in striatal IL-1β occurred after either sham-lesion or 6-OHDA lesion in AAV2-GFP rats. Although a greater increase in IL-1β was observed after 6-OHDA lesion in the IL-10 vector-treated group than in the control transgene group, there was no statistically significant difference between this response and that seen in sham-lesioned animals.

IL-1β may be neurotoxic to the nigrostriatal pathway *in vivo* only at very high tissue levels, similar to those seen after LPS exposure. Moderately elevated levels of IL-1β prior to 6-OHDA lesion may provide preconditioning-like neuroprotection through glial activation.[20,30] This would explain partial dopaminergic protection from 6-OHDA neurotoxicity reported in association with control transgene expression.[31] However, the control transgene used in our study did not elicit such protection. Our results appear to emphasize the importance of neurodegenerative mechanisms independent of proinflammatory cytokine signaling in the 6-OHDA model.

Both astroglia and microglia can be neuroprotective by, *e.g.*, secreting anti-inflammatory molecules such as IL-4 and IL-10. Our gene expression results suggest that increased IL-10 levels in the striatum produce an alteration in the initial astroglial response to 6-OHDA infusion. Expression of the astroglial calcium-binding protein SB100 was downregulated by IL-10, antagonizing the stimulatory effect of 6-OHDA on this gene. At micromolar concentrations *in vitro*, S100B is toxic and can produce neuronal apoptosis[32] by stimulating astrocytic inducible nitric oxide synthase expression and nitric oxide release.[33] This calcium-binding protein may prove to be a useful biomarker of disease progression for idiopathic PD, as there appears to be a positive association between clinical symptoms and serum S100B levels.[34]

Gene expression analyses revealed that the production of the chemokines CCL5 and CXCL13 was elevated in AAV2-hIL-10 versus control 6-OHDA rats at 3 days after the 6-OHDA lesion. CCL5 is produced by $CD8^+$ T cells, and it mainly recruits monocytes and T cells to the site of inflammation.[16,17,29,35] In contrast, CXCL13 is a chemokine that mainly attracts B cells to the inflamed central nervous system.[36,37] Normalization of carcinoembryonic antigen-related cell adhesion molecule 1 occurred in 6-OHDA rats that had received AAV2-hIL-10, in contrast to the control 6-OHDA rats. This endothelial adhesion factor has been shown to play a significant role in prolonging the presence of neutrophils during inflammatory responses. Neutrophils act quickly as a first line of defense in the neutralization of pathogens, in addition to inhibiting T-cell activation and promoting endothelial cell motility in rat brain.[38,39] Taken together, these changes suggest that lymphocytes and astroglia play important roles in the acute mechanisms involved in IL-10-mediated neuroprotection. However, it should be noted that these experiments do not take into consideration the nontranscriptional effects of IL-10.

This work represents the first demonstration of nigrostriatal neuroprotection by an AAV2 vector containing an IL-10 transgene in a rodent model of PD. It has been reported that this cytokine is capable of reducing dopaminergic neurodegeneration induced by acute inflammation when delivered as a recombinant protein directly into the brain.[8,40] Chronic, but not acute, delivery of IL-10 was sufficient to achieve this neuroprotection through a reduction of neuronal apoptosis, but the authors did not report on the markers of inflammation. The idea that inflammation may have a primary role in the pathology of PD, and is not merely a response to neurodegeneration, is a controversial one. This is partly because 6-OHDA, 1-methyl-4-phenyl-1,2,3, 6-tetrahydropyridine, and LPS, are all found to induce the microglial activation that precedes dopaminergic neurodegeneration, and reduction of such activation attenuates this effect.[41,42] Our work replicates this cause-and-effect relationship, but the attenuation of microglial activation by IL-10 does not result in the reduction of a key inflammatory cytokine IL-1β. Perhaps this explains why AAV2-hIL-10 did not provide complete neuroprotection against the toxic effects of 6-OHDA. This may also result from the fact that 6-OHDA has direct neurotoxic effects, independent of glial activation.[43,44] However, IL-10 did not provide complete protection of nigral dopaminergic neurons against LPS exposure either.[8] These observations suggest that microglial activation is not the only mechanism leading to cell death in these models. Further, our study showed that the level of protection was greater at the cell body than at the striatal terminals. This finding suggests that a longer period of IL-10 infusion may be required in the striatum prior to 6-OHDA lesion in order to protect the terminals. In addition, given that the model employed here involves a full lesion of the nigrostriatal pathway, the level of protection observed suggests its therapeutic value.

In summary, we have demonstrated that rats with enhanced nigrostriatal expression of IL-10 show decreased susceptibility to 6-OHDA-induced degeneration of dopaminergic nigrostriatal neurons. One mechanism by which this occurs involves the reduction of gliosis. Additional preclinical studies are warranted with this vector system in rodent models of PD, in order to evaluate the detailed mechanisms underlying its neuroprotective effects.

MATERIALS AND METHODS

Animals. Male Sprague–Dawley rats (Charles River Laboratories, Wilmington, MA; 200–250 g at the start of the study) were housed in the laboratory animal research center at University of California San Francisco. The rats were kept on a 12-hour light/dark cycle, and housed individually with free access to food and water.

AAV2-hIL10 production. The human IL-10 cDNA (accession number: NM000572) was cloned into an AAV2 shuttle plasmid, and a recombinant AAV2 containing hIL-10 under the control of the cytomegalovirus promoter was generated by a triple transfection technique and then purified by CsCl gradient centrifugation.[45,46] AAV2-hIL-10 was concentrated to ~1×10^{13} vector genomes/ml as determined by quantitative PCR. A virtually identical method was used for production of AAV2-green fluorescent protein (GFP), with GFP cDNA replacing hIL-10 cDNA.

Stereotactic surgery. Under surgical anesthesia (2% isoflurane, 2 l/min O_2), the animal was placed in a stereotactic frame. An incision was made in the skin overlying the skull and a burr-hole was made just above the infusion site. AAV2 vector (20 µl) was infused into the striatum at the following stereotactic coordinates: AP: +0.5, ML: −2.8 relative to bregma and DV: −5 mm relative to dura.[47] Three days prior to the 6-OHDA lesion, the rats were infused bilaterally with 1×10^{11} vector genomes of AAV2-hIL-10 or AAV2-GFP by CED. Viral vectors were infused at a sequential, ascending infusion rate (0.2, 0.5, and 0.8 µl/min) over a 40-minute period. The toxin, 6-OHDA hydrobromide (1 mg/ml in sterile saline containing 0.2% ascorbic acid), was infused unilaterally into the striatum in sequential, ascending infusion steps as described, and the cannula was left in place for 5 minutes before being retracted. After infusion, the scalp was closed with sutures. Fifty-six days after the lesion, a >97% depletion of striatal DA terminals was routinely found, associated with a loss of 80% of DA neurons of the SNc.[13]

Behavioral assessments. The rats were evaluated weekly for forelimb akinesia over a period of 28 days after intrastriatal infusion of 6-OHDA. In

the step-adjustment test,[15] the experimenter held the hindlimbs of the rat in place with one hand and used the other hand to restrain the forelimb that was not being tested. The paw to be assessed was allowed to touch the table. The number of adjusting steps was counted while the rat was moved sideways along the table; this was done in both the backhand and forehand directions. The cylinder test exploits the rat's innate drive to explore a novel environment.[48] Each rat was placed in a Lucite cylinder for a period of 5 minutes, and an experimenter who was blinded as to treatment group counted the number of full wall contacts made with the forepaws. At 28 days after infusion of 6-OHDA, the rats were assessed for apomorphine-induced (0.05 mg/kg subcutaneously) rotational behavior. This was monitored in automated rotometer bowls. The rats were allowed to acclimatize to the rotometry bowls for 60 minutes. Immediately after injection of apomorphine the animals were placed in the test bowl, and the number of rotations made either clockwise or counterclockwise was recorded over a test period of up to 2 hours.

Analyses of DA and metabolites using high-performance liquid chromatography. The rats were killed, the brains were removed, and 1-mm blocks of the striatum at the level of the anterior commissure were dissected followed by isolation of left and right striatum. These samples were placed immediately in a 1:20 ratio of wet-weight of tissue to 0.4 mol/l perchloric acid, sonicated, and centrifuged for 15 minutes at 14,000 rpm at 4 °C. The supernatant (30 µl) was injected onto a high-performance liquid chromatography system coupled to an electrochemical detection device (Coularray; ESA, Chelmsford, MA) for measuring DA and its metabolites, dihydroxyphenylacetic acid and homovanillic acid. The protein content was determined in pellet fractions by the method described by Lowry.[49]

Immunohistochemistry. Midbrain blocks containing the SNc were snap-frozen in 2-methyl butane and stored at −80 °C. The frozen blocks were cut into 20-µm sections on a cryostat. Prior to immunostaining, mounted sections were fixed in 4% paraformaldehyde phosphate-buffered saline at room temperature and washed in phosphate-buffered saline. Endogenous peroxidases were quenched in hydrogen peroxide (0.3% vol/vol). A separate group of rats was prepared for GFAP immunohistochemistry. Midbrain blocks were fixed overnight in 4% paraformaldehyde in phosphate-buffered saline at 4 °C, and then cryoprotected in sucrose before being stored at −80 °C. For immunohistochemical visualization of TH, MAC-1, or GFAP immunoreactivity, brain sections were incubated in a blocking solution of 10% normal rabbit serum, 10% normal horse serum, or 10% normal goat serum in superblock diluent (Scytek, Cache, UT), respectively. The sections were incubated overnight at 4 °C in polyclonal sheep anti-TH (1:500; Pelfreez Biologicals, Rogers, AR), mouse anti-rat MAC-1 (1:1,000; Serotec, Raleigh, NC), or rabbit anti-GFAP (1:5,000; Abcam, Cambridge, MA). The avidin–biotin immunoperoxidase method was used as a detection system (ABC Elite; Vector Laboratories, Burlingame, CA). Immunoreactivity was visualized using the chromagen 3,3′-diaminobenzidine and hydrogen peroxide.

A Leitz microscope and the Stereo Investigator program were used for counting TH-positive neurons in the SNc under a ×50 objective, in coronal sections that contained the medial terminal nucleus of the accessory optical tract (MT) that acts as a boundary between the SNc and the ventral tegmental area. In each treatment group, two sections per rat were analyzed for the number of TH-containing neurons in the SNc. MAC-1 immunoreactivity was visualized on sections of SNc adjacent to those used to test for TH immunoreactivity. GFAP staining was performed on every sixth section though the rostro-caudal axis of the SNc, and then rated by two experimenters who were blinded as to treatment groups. The following scale was employed: a score of 0 indicated the presence of resting astroglia, 1 indicated the presence of very few activated astrocytes, and a score between 2 and 4 indicated the extent of distribution, density, and morphology of the activated astroglia observed.

Enzyme-linked immunosorbent assays. The concentrations of rat IL-1β and human IL-10 were determined using commercially available Quantikine and Quantiglo kits, respectively (R & D Systems, Minneapolis, MN). The sensitivity of these kits was 15 pg/ml and 2 pg/ml, respectively. After dissection, the striata were stored at −80 °C. Samples were later homogenized with a model 100 Fisher Science Dismembrator in 250 µl of ice-cold buffer composed of 25 mmol/l Tris buffer (pH 7.4), 150 mmol/l NaCl, 2 mmol/l EDTA, and protease inhibitors (Complete Mini; Roche, Palo Alto, CA) and then centrifuged at 13,000 rpm for 15 minutes. The supernatants were collected and cytokine levels were detected using ELISA. Either standard kit control or samples were added to each well precoated with antibodies specific for rat IL-1β or human IL-10 for 2 and 3 hours, respectively. Samples were run in duplicate. After thorough washing of each well, enzyme-linked polyclonal antibodies against rat IL-1β or human IL-10 were added to each well and allowed to incubate for 2 hours. Next, the plates were washed and substrate solution (IL-1β Supersignal; hIL-10 kit substrate solution; Pierce, Milwaukee, WI) was added. The plates were read on a plate-reader at 10 and 40 minutes for IL-1β and hIL-10 ELISA's, respectively. Chemiluminescence was measured on a Flx800 microplate reader (Biotek, Winooski, VT) and expressed in relative light units.

Gene expression profiling. The striata were quickly dissected on wet ice and stored at −80 °C awaiting extraction of RNA with the Trizol purification kit (Invitrogen, Carlsbad, CA). RNA samples from the striatum were reverse transcribed and analyzed on the Affymetrix Rat Genome 230 2.0 representing 28,700 rat genes (Affymetrix, Santa Clara, CA). The Affymetrix chips were analyzed using the Array Assist software (Stratagene, La Jolla, CA). PLIER protocol was used for probe level analysis, and *t*-test was used for differential expression analysis. Gene expression levels were counted as "significantly changed" when mRNA levels between samples differed by more than twofold with $P < 0.05$. The following quality control criteria were used for the Affymetrix analysis: The 3′/5′ ratios for glyceraldehyde 3-phosphate dehydrogenase were to be <1.5; spiked-in controls were to have normal profiles; and principal component analysis on hybridization groups had to show appropriate clustering.

Quantitative PCR. PCR primer and TaqMan probe sequences were purchased from Applied Biosystems (Foster City, CA). PCR was conducted in triplicate with 20-ml reaction volumes of 1× TaqMan buffer (1× Applied Biosystems PCR buffer, 20% glycerol, 2.5% gelatin, 60 nmol/l Rox as a passive reference), 5.5 mmol/l $MgCl_2$, 0.5 mmol/l each primer, 0.2 mmol/l each deoxynucleotide triphosphate, 200 nmol/l probe, and 0.025 U/ml AmpliTaq Gold (Applied Biosystems) with 5 ng cDNA. A large master mix of these components (minus the primers, probe, and cDNA) was made for each experiment and aliquoted into individual tubes, one for each cDNA sample. cDNA was then added to the aliquoted master mix. The master mix with cDNA was aliquoted into a 384-well plate. The primers and probes were mixed together and added to the master mix and cDNA in the 384-well plate. PCR was conducted on the ABI 7900HT (Applied Biosystems) using the following cycle parameters: 1 cycle of 95° for 10 minutes, and 40 cycles of 95° for 15 seconds followed by 60° for 1 minute. Analysis was carried out using the SDS software (version 2.3; Applied Biosystems) supplied with the ABI 7900HT in order to determine the C_t (cycle threshold) values of each reaction.

C_t values were determined for three test reactions and three reference reactions in each sample. These values were averaged, and ΔC_t was calculated as [ΔC_t = C_t (test locus) − C_t (control locus)]. PCR efficiencies were measured for all custom assays and were ≥90%. Therefore the relative multiple of difference was calculated for each primer/probe combination as $2^{-\Delta C_t} \times 100$. The average C_t measurements were normalized to housekeeping gene expression (rat glyceraldehyde 3-phosphate dehydrogenase) using the formula:

ΔC_t = average C_t (gene of interest) − average (C_t glyceraldehyde 3-phosphate dehydrogenase)

Statistical analysis. Initially the data were analyzed using a two-way analysis of variance (Prism Graphpad, La Jolla, CA). Wherever a significant effect in one of the experimental variables was observed, one-way analysis of variance was employed to examine more closely the effect of treatment on the variable. Where significance was revealed, *post hoc* comparisons were made using Newman–Keuls or Bonferroni tests. Differences between left and right sides were evaluated using Student's paired *t*-tests; intergroup comparisons were made with independent *t*-tests. Gene array and quantitative reverse transcriptase PCR data were analyzed using independent *t*-tests.

ACKNOWLEDGMENTS

We thank Katherine High, Fraser Wright, and Shangzhen Zhou at Children's Hospital of Philadelphia for their generous gift of AAV2-hIL-10. This work was supported in part by a generous gift from Avigen Inc., and also by a grant from the National Institutes of Health to K.S.B. Also, we acknowledge the Genome Analysis Core Facility, Helen Diller Family Comprehensive Cancer Center, University of California San Francisco, for performing the confirmation quantitative reverse transcriptase PCR assays.

REFERENCES

1. Nagatsu, T and Sawada, M (2006). Cellular and molecular mechanisms of Parkinson's disease: neurotoxins, causative genes, and inflammatory cytokines. *Cell Mol Neurobiol* **26**: 781–802.
2. Zhang, W, Wang, T, Pei, Z, Miller, DS, Wu, X, Block, ML *et al.* (2005). Aggregated alpha-synuclein activates microglia: a process leading to disease progression in Parkinson's disease. *FASEB J* **19**: 533–542.
3. Su, X, Maguire-Zeiss, KA, Giuliano, R, Prifti, L, Venkatesh, K and Federoff, HJ (2007). Synuclein activates microglia in a model of Parkinson's disease. *Neurobiol Aging* (epub ahead of print).
4. Griffin, WS, Liu, L, Li, Y, Mrak, RE and Barger, SW (2006). Interleukin-1 mediates Alzheimer and Lewy body pathologies. *J Neuroinflammation* **3**: 5.
5. Wu, DC, Jackson-Lewis, V, Vila, M, Tieu, K, Teismann, P, Vadseth, C *et al.* (2002). Blockade of microglial activation is neuroprotective in the 1-methyl-4-phenyl-1,2,3,6-tetrahydropyridine mouse model of Parkinson disease. *J Neurosci* **22**(5): 1763–1771.
6. Molina-Holgado, E, Vela, JM, Arevalo-Martin, A and Guaza, C (2001). LPS/IFN-gamma cytotoxicity in oligodendroglial cells: role of nitric oxide and protection by the anti-inflammatory cytokine IL-10. *Eur J Neurosci* **13**: 493–502.
7. Lynch, AM, Walsh, C, Delaney, A, Nolan, Y, Campbell, VA and Lynch, MA (2004). Lipopolysaccharide-induced increase in signalling in hippocampus is abrogated by IL-10--a role for IL-1 beta? *J Neurochem* **88**: 635–646.
8. Arimoto, T, Choi, DY, Lu, X, Liu, M, Nguyen, XV, Zheng, N *et al.* (2007). Interleukin-10 protects against inflammation-mediated degeneration of dopaminergic neurons in substantia nigra. *Neurobiol Aging* **28**: 894–906.
9. Qian, L, Block, ML, Wei, SJ, Lin, CF, Reece, J, Pang, H *et al.* (2006). Interleukin-10 protects lipopolysaccharide-induced neurotoxicity in primary midbrain cultures by inhibiting the function of NADPH oxidase. *J Pharmacol Exp Ther* **319**: 44–52.
10. Pestka, S, Krause, CD and Walter, MR (2004). Interferons, interferon-like cytokines, and their receptors. *Immunol Rev* **202**: 8–32.
11. Qin, L, Block, ML, Liu, Y, Bienstock, RJ, Pei, Z, Zhang, W *et al.* (2005). Microglial NADPH oxidase is a novel target for femtomolar neuroprotection against oxidative stress. *FASEB J* **19**: 550–557.
12. Sauer, H and Oertel, WH (1994). Progressive degeneration of nigrostriatal dopamine neurons following intrastriatal terminal lesions with 6-hydroxydopamine: a combined retrograde tracing and immunocytochemical study in the rat. *Neuroscience* **59**: 401–415.
13. Oiwa, Y, Sanchez-Pernaute, R, Harvey-White, J and Bankiewicz, KS (2003). Progressive and extensive dopaminergic degeneration induced by convection-enhanced delivery of 6-hydroxydopamine into the rat striatum: a novel rodent model of Parkinson disease. *J Neurosurg* **98**: 136–144.
14. Andersen, SR, Lambrecht, LJ, Swan, SK, Cutler, DL, Radwanski, E, Affrime, MB *et al.* (1999). Disposition of recombinant human interleukin-10 in subjects with various degrees of renal function. *J Clin Pharmacol* **39**: 1015–1020.
15. Olsson, M, Nikkhah, G, Bentlage, C and Bjorklund, A (1995). Forelimb akinesia in the rat Parkinson model: differential effects of dopamine agonists and nigral transplants as assessed by a new stepping test. *J Neurosci* **15**: 3863–3875.
16. Owais, M and Arya, SK (1999). Antiviral chemokines: intracellular life of recombinant C-C chemokine RANTES. *J Hum Virol* **2**: 270–282.
17. Yano, S, Mentaverri, R, Kanuparthi, D, Bandyopadhyay, S, Rivera, A, Brown, EM *et al.* (2005). Functional expression of beta-chemokine receptors in osteoblasts: role of regulated upon activation, normal T cell expressed and secreted (RANTES) in osteoblasts and regulation of its secretion by osteoblasts and osteoclasts. *Endocrinology* **146**: 2324–2335.
18. Raponi, E, Agenes, F, Delphin, C, Assard, N, Baudier, J, Legraverend, C *et al.* (2007). S100B expression defines a state in which GFAP-expressing cells lose their neural stem cell potential and acquire a more mature developmental stage. *Glia* **55**: 165–177.
19. Kirik, D, Rosenblad, C and Bjorklund, A (1998). Characterization of behavioral and neurodegenerative changes following partial lesions of the nigrostriatal dopamine system induced by intrastriatal 6-hydroxydopamine in the rat. *Exp Neurol* **152**: 259–277.
20. Saura, J, Pares, M, Bove, J, Pezzi, S, Alberch, J, Marin, C *et al.* (2003). Intranigral infusion of interleukin-1beta activates astrocytes and protects from subsequent 6-hydroxydopamine neurotoxicity. *J Neurochem* **85**: 651–661.
21. Cicchetti, F, Brownell, AL, Williams, K, Chen, YI, Livni, E and Isacson, O (2002). Neuroinflammation of the nigrostriatal pathway during progressive 6-OHDA dopamine degeneration in rats monitored by immunohistochemistry and PET imaging. *Eur J Neurosci* **15**: 991–998.
22. Langston, JW, Forno, LS, Tetrud, J, Reeves, AG, Kaplan, JA and Karluk, D (1999). Evidence of active nerve cell degeneration in the substantia nigra of humans years after 1-methyl-4-phenyl-1,2,3,6-tetrahydropyridine exposure. *Ann Neurol* **46**: 598–605.
23. McGeer, PL, Schwab, C, Parent, A and Doudet, D (2003). Presence of reactive microglia in monkey substantia nigra years after 1-methyl-4-phenyl-1,2,3,6-tetrahydropyridine administration. *Ann Neurol* **54**: 599–604.
24. Czlonkowska, A, Kohutnicka, M, Kurkowska-Jastrzebska, I and Czlonkowski, A (1996). Microglial reaction in MPTP (1-methyl-4-phenyl-1,2,3,6-tetrahydropyridine) induced Parkinson's disease mice model. *Neurodegeneration* **5**: 137–143.
25. Iravani, MM, Leung, CC, Sadeghian, M, Haddon, CO, Rose, S and Jenner, P (2005). The acute and the long-term effects of nigral lipopolysaccharide administration on dopaminergic dysfunction and glial cell activation. *Eur J Neurosci* **22**: 317–330.
26. Youdim, MB, Stephenson, G and Ben Shachar, D (2004). Ironing iron out in Parkinson's disease and other neurodegenerative diseases with iron chelators: a lesson from 6-hydroxydopamine and iron chelators, desferal and VK-28. *Ann NY Acad Sci* **1012**: 306–325.
27. Block, ML, Wu, X, Pei, Z, Li, G, Wang, T, Qin, L *et al.* (2004). Nanometer size diesel exhaust particles are selectively toxic to dopaminergic neurons: the role of microglia, phagocytosis, and NADPH oxidase. *FASEB J* **18**: 1618–1620.
28. Wirjatijasa, F, Dehghani, F, Blaheta, RA, Korf, HW, Hailer, NP (2002). Interleukin-4, interleukin-10, and interleukin-1-receptor antagonist but not transforming growth factor-beta induce ramification and reduce adhesion molecule expression of rat microglial cells. *J Neurosci Res* **68**: 579–587.
29. Gelderblom, H, Londono, D, Bai, Y, Cabral, ES, Quandt, J, Hornung, R *et al.* (2007). High production of CXCL13 in blood and brain during persistent infection with the relapsing fever spirochete Borrelia turicatae. *J Neuropathol Exp Neurol* **66**: 208–217.
30. Sharma, V, Mishra, M, Ghosh, S, Tewari, R, Basu, A, Seth, P *et al.* (2007). Modulation of interleukin-1beta mediated inflammatory response in human astrocytes by flavonoids: implications in neuroprotection. *Brain Res Bull* **73**: 55–63.
31. Gerin, C (2002). Behavioral improvement and dopamine release in a Parkinsonian rat model. *Neurosci Lett* **330**: 5–8.
32. Zimmer, DB, Cornwall, EH, Landar, A and Song, W (1995). The S100 protein family: history, function, and expression. *Brain Res Bull* **37**: 417–429.
33. Hu, J, Ferreira, A and Van Eldik, LJ (1997). S100beta induces neuronal cell death through nitric oxide release from astrocytes. *J Neurochem* **69**: 2294–2301.
34. Schaf, DV, Tort, AB, Fricke, D, Schestatsky, P, Portela, LV, Souza, DO *et al.* (2005). S100B and NSE serum levels in patients with Parkinson's disease. *Parkinsonism Relat Disord* **11**: 39–43.
35. Castellani, ML, Shanmugham, LN, Petrarca, C, Simeonidou, I, Frydas, S, De Colli, M *et al.* (2007). Expression and secretion of RANTES (CCL5) in granulomatous calcified tissue before and after lipopolysaccharide treatment *in vivo. Calcif Tissue Int* **80**: 60–67.
36. Ransohoff, RM, Kivisakk, P and Kidd, G (2003). Three or more routes for leukocyte migration into the central nervous system. *Nat Rev Immunol* **3**: 569–581.
37. Kim, CH, Rott, LS, Clark-Lewis, I, Campbell, DJ, Wu, L and Butcher, EC (2001). Subspecialization of CXCR5+ T cells: B helper activity is focused in a germinal center-localized subset of CXCR5+ T cells. *J Exp Med* **193**: 1373–1381.
38. Nagaishi, T, Pao, L, Lin, SH, Iijima, H, Kaser, A, Qiao, SW et al. (2006). SHP1 phosphatase-dependent T cell inhibition by CEACAM1 adhesion molecule isoforms. *Immunity* **25**: 769–781.
39. Muller, MM, Singer, BB, Klaile, E, Obrink, B, Lucka, L (2005). Transmembrane CEACAM1 affects integrin-dependent signaling and regulates extracellular matrix protein-specific morphology and migration of endothelial cells. *Blood* **105**: 3925–3934.
40. Qian, L, Hong, JS, Flood, PM (2006). Role of microglia in inflammation-mediated degeneration of dopaminergic neurons: neuroprotective effect of interleukin 10. *J Neural Transm Suppl* **70**: 367–371.
41. He, Y, Appel, S and Le, W (2001). Minocycline inhibits microglial activation and protects nigral cells after 6-hydroxydopamine injection into mouse striatum. *Brain Res* **909**: 187–193.
42. Sriram, K, Matheson, JM, Benkovic, SA, Miller, DB, Luster, MI and O'Callaghan, JP (2006). Deficiency of TNF receptors suppresses microglial activation and alters the susceptibility of brain regions to MPTP-induced neurotoxicity: role of TNF-alpha. *FASEB J* **20**: 670–682.
43. Dehmer, T, Lindenau, J, Haid, S, Dichgans, J and Schulz, JB (2000). Deficiency of inducible nitric oxide synthase protects against MPTP toxicity *in vivo. J Neurochem* **74**: 2213–2216.
44. Block, ML and Hong, JS (2005). Microglia and inflammation-mediated neurodegeneration: multiple triggers with a common mechanism. *Prog Neurobiol* **76**: 77–98.
45. Matsushita, T, Elliger, S, Elliger, C, Podsakoff, G, Villarreal, L, Kurtzman, GJ *et al.* (1998). Adeno-associated virus vectors can be efficiently produced without helper virus. *Gene Ther* **5**: 938–945.
46. Wright, JF, Qu, G, Tang, C and Sommer, JM (2003). Recombinant adeno-associated virus: formulation challenges and strategies for a gene therapy vector. *Curr Opin Drug Discov Devel* **6**: 174–178.
47. Paxinos, G and Watson, C (1982). The Rat brain in stereotaxic coordinates. Academic Press: New York.
48. Cenci, MA, Whishaw, IQ and Schallert, T (2002). Animal models of neurological deficits: how relevant is the rat? *Nat Rev Neurosci* **3**: 574–579.
49. Lowry, OH, Rosebrough, NJ, Farr, AL and Randall, RJ (1951). Protein measurement with the Folin phenol reagent. *J Biol Chem* **193**: 265–275.
50. Zheng, JS, Tang, LL, Zheng, SS, Zhan, RY, Zhou, YQ, Goudreau, J *et al.* (2005). Delayed gene therapy of glial cell line-derived neurotrophic factor is efficacious in a rat model of Parkinson's disease. *Brain Res Mol Brain Res* **134**: 155–161.